ADVANCED MATERIALS

Supporting Information

for *Adv. Mater.,* DOI: 10.1002/adma.202206593

Acoustic Crystallization of 2D Colloidal Crystals

*Johannes Menath, Reza Mohammadi, Jens Christian Grauer, Claudius Deters, Maike Böhm, Benno Liebchen, Liesbeth M. C. Janssen, Hartmut Löwen, and Nicolas Vogel**

Acoustic Crystallization of 2D Colloidal Crystals
Supplementary Information

Johannes Menath[a], Reza Mohammadi[a], Jens Christian Grauer[b], Claudius Deters[b], Maike Böhm[a], Benno Liebchen[c], Liesbeth M. C. Janssen[d], Hartmut Löwen[b] and Nicolas Vogel[a,*]

[a] Institute of Particle Technology, Friedrich-Alexander University Erlangen-Nürnberg, Cauerstrasse 4, 91058 Erlangen, Germany
[b] Institute for Theoretical Physics II: Soft Matter, Heinrich-Heine University Düsseldorf, D-40225 Düsseldorf, Germany
[c] Institute of Physics: Theory of Soft Matter, Technical University of Darmstadt, Hochschulstraße 12, 64289 Darmstadt, Germany
[d] Soft Matter and Biological Physics, Department of Applied Physics, Eindhoven University of Technology, 5600 MB Eindhoven, The Netherlands

A guide for experimentalists

The ideal sound parameters for monolayer annealing are dependent on the applied setup. They change with varying resonance conditions of the beaker and thus its diameter and the quantity of water it contains. The speaker type also plays an important role for excitement of sufficiently strong waves. As the particle movement can be observed visually when the right lighting conditions are applied (illumination should be placed on the interface and observation performed in specular reflection of this illuminated light), the acoustic parameters required to induce grain growth can be easily determined for arbitrary geometries, system sizes and equipment. In order to find the right annealing conditions for a given speaker-beaker-particle combination, it is advisable to take the following defined steps. As frequency and amplitude of the speaker both influence the motion of the interface, one parameter (preferably the frequency) should be fixed first before varying the others. The frequency should be chosen in so that a variation of amplitude results in a transition of almost no visible motion of the interface in the respective setup to a gentle motion and finally a splashing of water out of the beaker at the highest amplitude. Next, the surface coverage is probed, as it is the least sensitive parameter, yielding good results over a large surface coverage range. In order to find the right conditions, a high surface coverage monolayer should be initially produced and brought into motion with sound that induces waves of the water surface of about 3 mm height. No motion of the particles should be visible at this stage. By using a peristaltic pump, subsequently particles are sucked from the interface in order to slowly decrease the surface coverage. At one point, particle motion can be detected as surface coverage got sufficiently low. This condition should be used for a variation of amplitude, starting at low amplitudes, increasing them in small time steps. At some point a rearrangement and growth of crystal grains should be visible, indicating that efficient annealing conditions have been found. Finally, surface coverage, amplitude and frequency can be iterated to yield optimal results. By using this routine, suitable annealing parameters for a new system can be found within a view hours. In typical annealing experiments with such optimized conditions, the crystal grains grew rapidly and the quality of the sample increases with in the first 20-30s to the maximal level of order achievable by the conditions.

Theory for the optimal amplitude and for the optimal frequency

In the following we propose a simple theory for the optimal amplitude and for the optimal frequency needed to achieve an optimal grain annealing.

We first address a theory for the optimal amplitude. The relaxation of defects is complex in general but one decisive part is single vacancy hopping. We assume that vacancy hopping constitutes a key ingredient for complex defect annealing which largely determines the parameter dependence of the process. In detail, in order to make vacancy hopping in the solid possible, a particle has to jump over an energetic barrier made by all its surrounding neighbors in its cage, see Figure S7a. For fixed neighbors on a perfect hexagonal lattice the energetic barrier ΔE can simply be computed by a sum of the pairwise interactions for a particle located at a position $r_0 = xe_x$ on its way to fill a vacancy at the origin. In detail, upon acoustic annealing this energetic barrier is oscillating as a function of time t, as all particle distances are expanded, and is explicitly given by

$$\Delta E(t) = \max_x \sum_n U(r_n(x,t)) \qquad \text{(SI 1)}$$

where $U(r)$ is a pair potential as a function of distance r and the sum over n extends over all lattice positions except for the hopping particle and the vacancy. Here,
$r_n(x,t) = \|R_n(t) - xe_x\|$, where
$R_1(t) = d(t)\begin{pmatrix}1/2\\ \sqrt{3}/2\end{pmatrix}, R_2(t) = d(t)\begin{pmatrix}1/2\\ -\sqrt{3}/2\end{pmatrix}, R_3(t) = d(t)\begin{pmatrix}-1/2\\ \sqrt{3}/2\end{pmatrix}, \ldots$
are the positions of the neighboring particles at a given time t with
$d(t) = d_0(1 + A(1 - \cos(2\pi f t)))$ denoting the time dependent lattice constant of the breathing solid. The minimal value of $d(t)$ is the initial distance d_0. An example of the energetic barrier as a function of time is shown in Figure S7b. When the system is expanded most, the energetic barrier becomes minimal and that is the moment where vacancy hopping (or particle hopping) is most likely. If the minimal barrier height $\min_t \Delta E(t)$ is much larger than the thermal energy $k_B T$ the particle will not be able to overcome the barrier by thermal fluctuations such that the vacancy stays immobile. In the opposite case, when the barrier height is much smaller than $k_B T$, thermal fluctuations will strongly disturb the solid and create new defects. Therefore the optimal case for defect annealing occurs when the condition

$$\min_t \Delta E(t) \approx k_B T \qquad \text{(SI 2)}$$

is fulfilled. This establishes an implicit condition for the optimal amplitude. For repulsive interactions, such as the Yukawa potential used in this work, $\min_t \Delta E(t)$ increases with density such that the optimal amplitude is getting larger for increasing density. In fact the theory not only gives a prediction for varying density and particle size but also describes the experimental and simulation data reasonably well. An example for the criterion (SI 2) is shown in Figure S7c for the experimental parameters. The theory yields an optimal amplitude of 0.19 which is close to the simulated value of 0.22 (see Fig. 6a).

Regarding the optimal frequency, for sufficiently high amplitudes, high frequencies lead to particle oscillations still confining the particles to their lattice positions while low frequencies are likely to support the emergence of new defects. Optimality is expected when the frequency is comparable to the inverse Brownian timea^2/D_0needed for a single particle to diffuse over a distance a (lattice constant). It has then enough time to sample its surrounding to search for an escape route making defect annealing possible. Hence the optimal frequency ω_{opt} is approximately given by

$$\omega_{opt} \approx D_0/a^2 \qquad \text{(SI 3)}$$

This yields a scaling of the optimal frequency which is linear in the particle density ρ as ρ is proportional to a^{-2}. With the Stokes-Einstein relation $D_0 = \frac{k_B T}{6\pi\eta_s R}$ this expression (SI 3) also yields a simple scaling of ω_{opt} with the inverse particle radius R. For the experimental parameters the expression (SI 3) predicts an optimal frequency of 0.5/s which is the same order of magnitude as the simulated value of 1.5/s (see Fig. 6b).

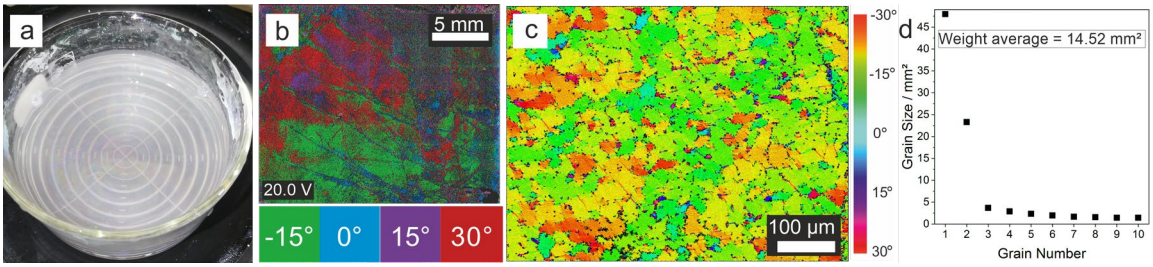

Figure S1: Destroyed monolayer at 8 Hz, η = 88 % and 20 V. a) Photograph of the monolayer after treatment with 8 Hz and 20 V. b) LIA image of the monolayer in (a). c) Size of the ten largest grains in image (b). d) A rigorous analysis of the crystal reveals a disturbed orientation at the microscale and a large loss of particles to the subphase (evidenced by the whitish appearance).

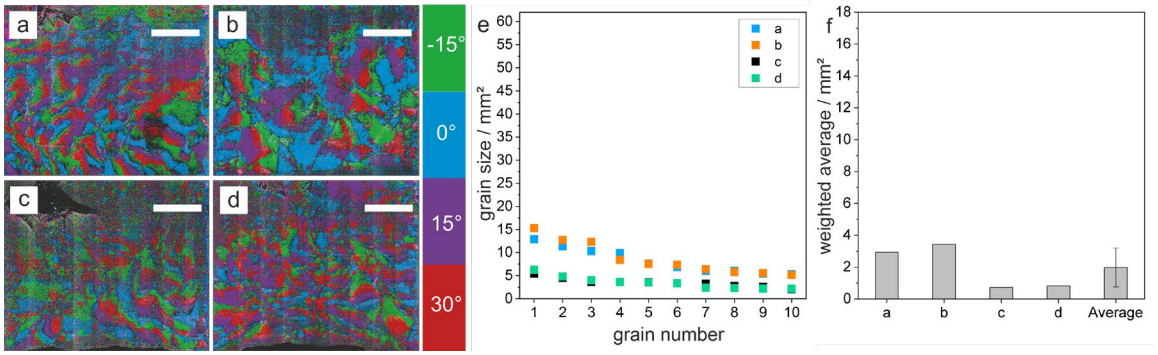

Figure S2: Reproducibility of the pure monolayer assembly at the air/water interface. a-d) LIA images of the pure monolayer without annealing. e) Size of the ten largest grains of the analyzed images (a-d). f) Weighted average of the grain sizes of the individual images and an overall average with standard deviation indicated. Sale bar: 5 mm.

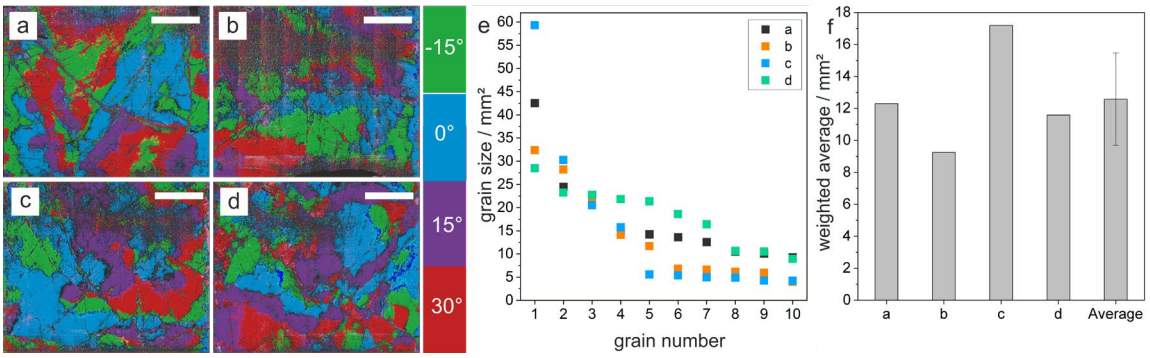

Figure S3: Reproducibility of the ACDC process using 16.5 V, 4 Hz and η = 88 %. a-d) LIA images of the monolayer after one minute of annealing. e) Size of the ten largest grains of the analyzed images (a-d). f) Weighted average of the grain sizes of the individual images and an overall average with standard deviation indicated. Scale bar: 5 mm.

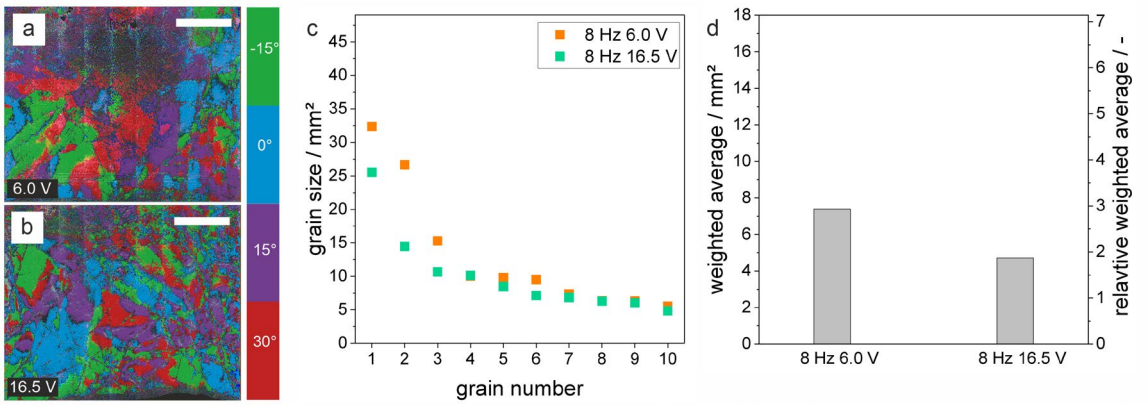

Figure S4: Annealing at 8 Hz and η = 88%. a) LIA image of a monolayer annealed at 8 Hz and 6 V. b) LIA image of a monolayer annealed at 8 Hz and 16.5 V. c) Sizes of the ten largest grains of the images (a) and (b). d) Average grain size of the images (a) and (b). Scale bar: 5 mm. Comparing Figure S4 to the data in Figure 2 shows that optimal amplitude and frequency are coupled: While an amplitude of 16.5 V at 4Hz increases the grain size by a factor of 6.2 (Figure 2), the same amplitude only leads to an increase by a factor of 2.4 at 8 Hz. At this higher frequency a lower amplitude of 6 V provides a more efficient annealing.

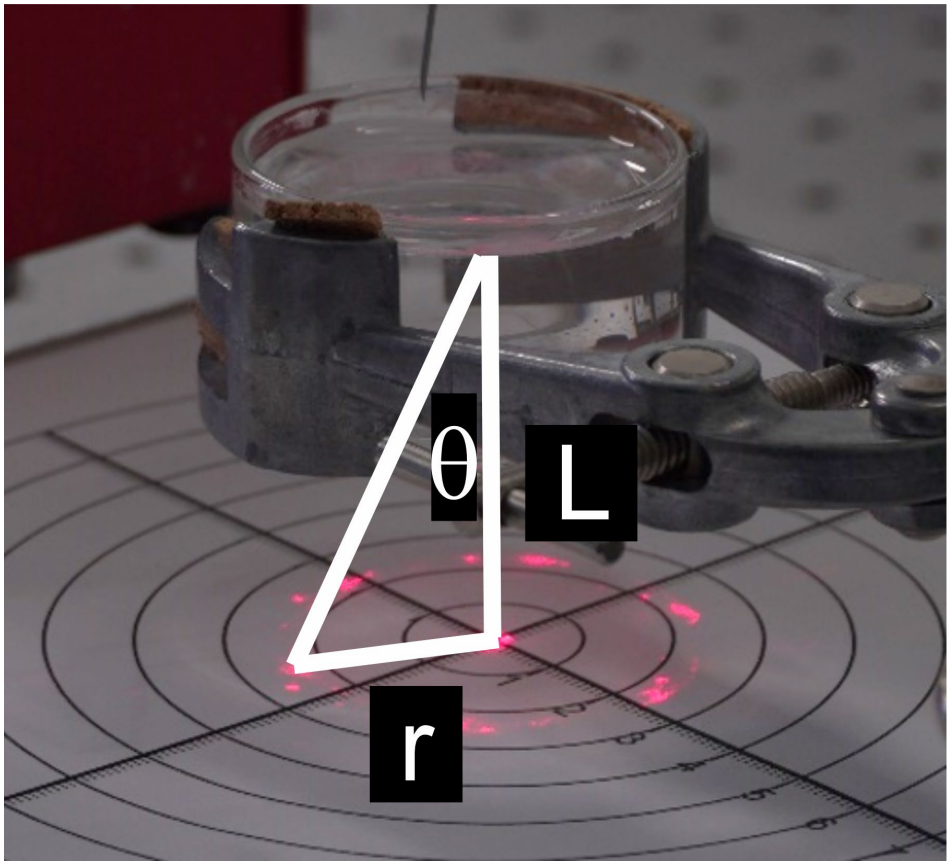

Figure S5: Illustration of the laser diffraction experiments where L is the distance between the diffraction pattern and the monolayer, r the diffraction radius and θ the angle between r and L.

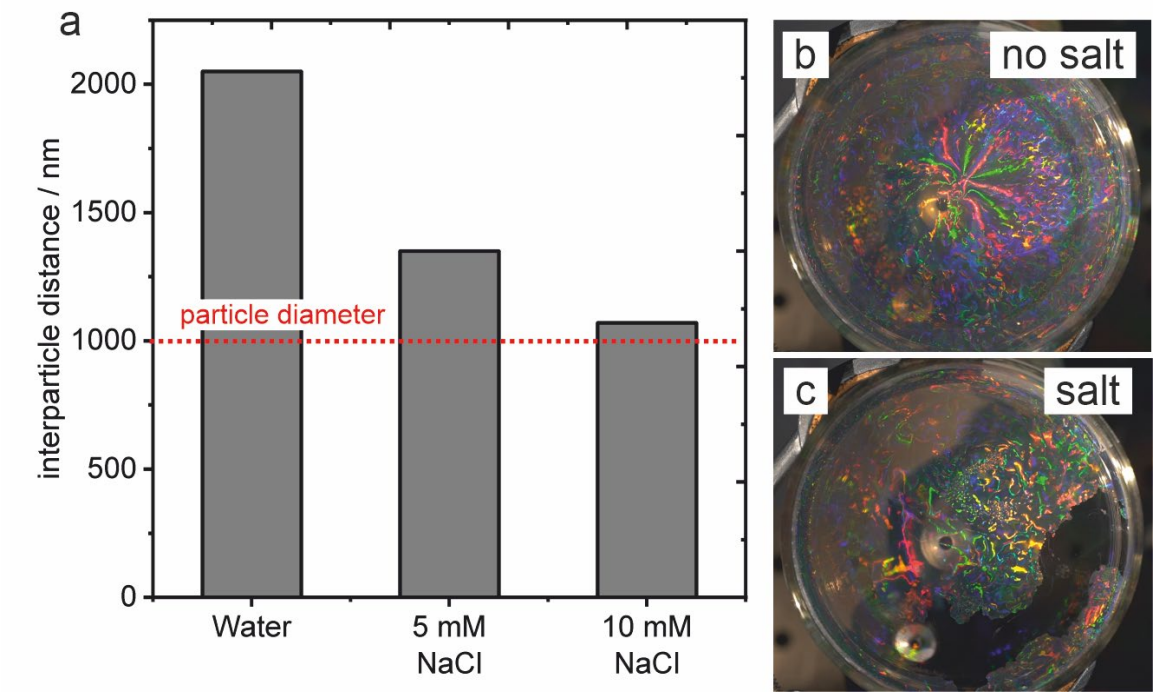

Figure S6: Sodium chloride addition to polystyrene monolayer. a) Interparticle distance versus salt concentration. b) Photograph of the monolayer without salt. b) Photograph of the monolayer with 10 mM NaCl in the subphase. A hole is visible which results from the decreasing inter particle distance.

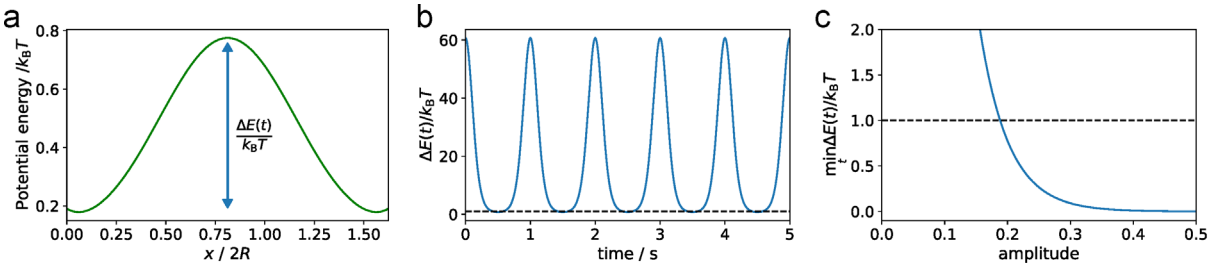

Figure S7: (a) Potential energy landscape which the particle has to overcome during vacancy hopping with an energetic barrier ΔE experienced by a particle that exchanges its position with a vacancy along a position coordinate x. (b) Energetic barrier as a function of time for breathing solid. The dashed line indicates the case when the potential energy barrier equals k_BT. (c) Minimal energetic barrier as a function of driving amplitude. The criterion for the optimal amplitude is indicated by the dashed line. The parameters are: D = 0.43µm^{2}s^{-1}, η = 74 %, A = 0.2(a,b), f = 1 Hz, V_0/γ = 3 × 10^5 µm^{3}s^{-1}, λ = 0.1µm using the Yukawa potential described in the main manuscript.

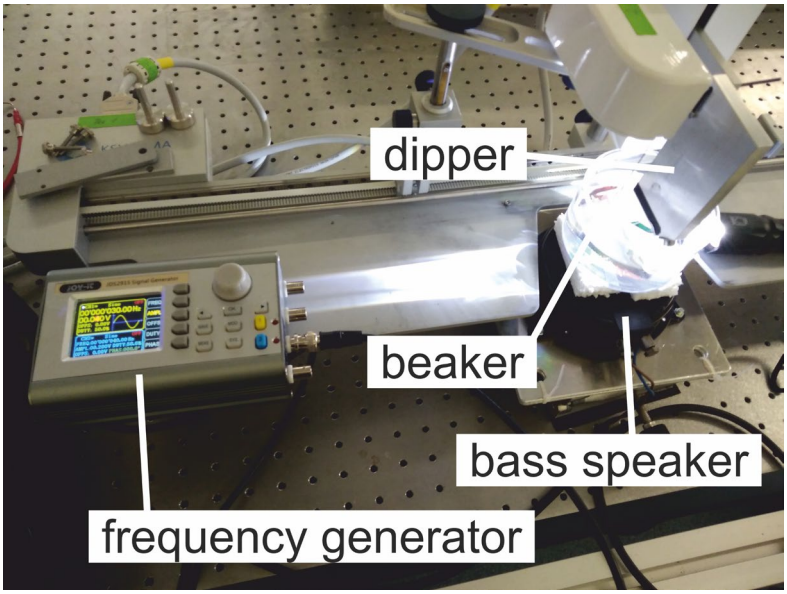

Figure S8: Second setup with labeled components. A d=9.4 cm beaker filled with 200 mL of MilliQ-water was placed on the bass speaker bass pump 4 Ω 50W by Sinus Line with two h = 2 cm foamed polystyrene dampeners between speaker and beaker. The dipper was used to deposit the monolayer.

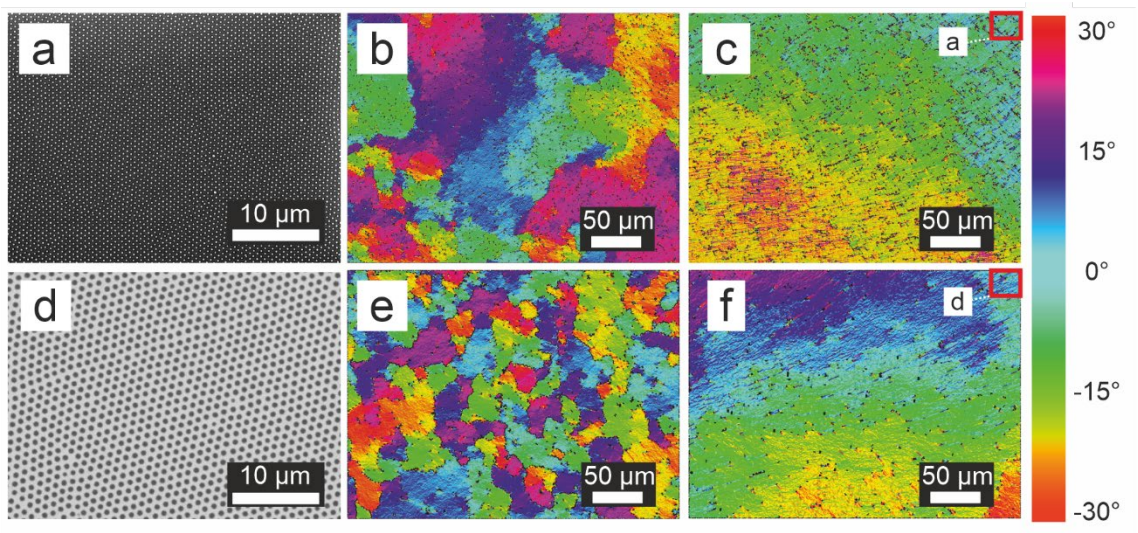

Figure S9: Particle tracking analysis for microgels and core-shell particles. a) Scanning electron micrograph of a hard core-soft shell particle lattice recorded at 5 keV. b-c) Color coded mosaic SEM images of a core-shell particle monolayer before (b) and after (c) sound application. d) Scanning electron micrograph of a microgel lattice recorded at 1 keV. e-f) Color coded mosaic SEM images of a microgel monolayer before (b) and after (c) sound application.

Supplementary Videos

Supplementary Movie 1: ACDC process using an amplitude ramp to 16.5 V, a frequency of 4 Hz, η=83% and d=1µm PS particles.

Supplementary Movie 2: Cycling between ordered and disordered monolayers at 4Hz and 80 Hz respectively and 16.5V, η=80% and d=1µm PS particles.

Supplementary Movie 3: Monolayer annealing of d=1µm PS particles at η=80% playing Beethoven's symphony no. 5 through the speaker with post-processed video sound. Music released under Creative Commons License CC0. Performed by Berliner Philharmoniker, conducted by Herbert von Karajan, Deutsche Grammophon 1962.

Supplementary Movie 3b: Monolayer annealing of d=1µm PS particles at η=80% playing Beethoven's symphony no. 5 through the speaker with original video sound.

Supplementary Movie 4: Monolayer annealing by stroking the rim of a wine glass filled with a PS d=1µm monolayer.

Supplementary Movie 5: Monolayer formation in the laser diffraction setup.

Supplementary Movie 6: Laser diffraction pattern during monolayer formation.

Supplementary Movie 7: Deposition of the d=1µm PS particle monolayer without NaCl in the sub phase to a glass slide at η=100%. No permanent gap opens up upon deposition.

Supplementary Movie 8: Salt addition in five steps to a final sub phase NaCl concentration of 10mM to a monolayer of d=1µm PS particles at η=82%. A hole opens up upon salt addition and particles added to a salt containing sub phase do not crystallize.

Supplementary Movie 9: Deposition of the d=1μm PS particle monolayer with 10mM NaCl in the sub phase to a glass slide at η=100%. A permanent gap opens up upon deposition.

Supplementary Movie 10: Simulation shown in Figure 7a. Annealing of a point defect.

Supplementary Movie 11: Simulation shown in Figure 7b. Crystal realignment with 30° of initial phase angle mismatch.

Supplementary Movie 12: Simulation shown in Figure 7c. Crystal realignment with 10° of initial phase angle mismatch.

Supplementary Movie 13: Simulation shown in Figure 7d. Crystal realignment with 5° of initial phase angle mismatch.